Superior sensitivity of novel molecular imaging probe: simultaneously targeting two types of endothelial injury markers

Dawei Sun,*,† Shintaro Nakao,* Fang Xie,* Souska Zandi,* Alexander Schering,* and Ali Hafezi-Moghadam,*,[1]

*Angiogenesis Laboratory, Massachusetts Eye and Ear Infirmary, Department of Ophthalmology, Harvard Medical School, Boston, Masachusetts, USA; †Department of Ophthalmology, Second Affiliated Hospital of Harbin Medical University, Harbin, China

ABSTRACT **The need remains great for early diagnosis of diseases. The special structure of the eye provides a unique opportunity for noninvasive light-based imaging of fundus vasculature. To detect endothelial injury at the early and reversible stage of adhesion molecule up-regulation, we generated novel imaging agents that target two distinct types of endothelial molecules, a mediator of rolling, P-selectin, and one that mediates firm adhesion, ICAM-1. Interactions of these double-conjugated fluorescent microspheres (MSs) in retinal or choroidal microvasculature were visualized in live animals by scanning laser ophthalmoscopy. The new imaging agents showed significantly higher sensitivity for detection of endothelial injury than singly conjugated MSs (rPSGL-1- or α-ICAM-1-conjugated), both in terms of rolling ($P<0.01$) and firm adhesion ($P<0.01$). The rolling flux of α-ICAM-1-conjugated MSs did not differ in EIU animals, whereas double-conjugated MSs showed significantly higher rolling flux ($P<0.01$), revealing that ICAM-1 *in vivo* supports rolling, once MS interaction with the endothelium is initiated. Double-conjugated MSs specifically detected firmly adhering leukocytes ($P<0.01$), allowing *in vivo* quantification of immune response. Antiinflammatory treatment with dexamethasone led to reduced leukocyte accumulation ($P<0.01$) as well as MS interaction ($P<0.01$), which suggests that treatment success and resolution of inflammation is quantitatively reflected with this molecular imaging approach. This work introduces novel imaging agents for noninvasive detection of endothelial injury *in vivo*. Our approach may be developed further to diagnose human disease at a much earlier stage than currently possible.—Sun, D., Nakao, S., Xie, F., Zandi, S., Schering, A., Hafezi-Moghadam, A. Superior sensitivity of novel molecular imaging probe: simultaneously targeting two types of endothelial injury markers. *FASEB J.* 24, 1532–1540 (2010). www.fasebj.org**

Key Words: early diagnosis · ocular inflammation · leukocyte-endothelial interaction · adhesion molecules

OCULAR INFLAMMATORY DISEASES, such as uveitis, cause severe visual loss (1). Uveitis can affect any part of the eye, including the retina and choroid, and is characterized by the accumulation of leukocytes in ocular tissues (2). Early detection of ocular vascular injury would help to establish the diagnosis, whereupon effective treatments such as corticosteroids could halt inflammation before irreversible structural damages occur.

In vivo visualization techniques of the choroidal microcirculation, including conventional fluorescein angiography (FA) and indocyanine green angiography (ICGA) or the experimental laser-targeted angiography (3, 4), are used to investigate the choroidal vascular network and hemodynamic conditions (5). However, these methods do not allow evaluation of leukocyte-endothelial interaction in the retinal and choriocapillaris flow or identification of specific molecular changes during disease. Recently, we introduced a novel technique for detection of endothelial surface molecules in acute ocular inflammation (6). Using adhesion-molecule-conjugated fluorescent microspheres (MSs) (7) in live animals, we showed early endothelial changes in ocular microvessels at an early stage, which were previously detectable only by the most sensitive *in vitro* techniques, such as immunohistochemistry or PCR (6). To cause vascular injury, we used endotoxin-induced uveitis (EIU), an established animal model of acute ocular inflammation (8). In this model, a footpad injection of lipopolysaccharide (LPS), a component of gram-negative bacterial cell wall, causes pronounced ocular inflammation (2, 8).

Our imaging approach is founded on certain aspects of leukocyte-endothelial interaction, a common component in the pathogenesis of various ocular diseases. Leukocytes normally do not interact with the endothelium of blood vessels, save for occasional tethering. However, at sites of inflammation, endothelial cells express adhesion molecules, such as P-selectin and intercellular adhesion molecule-1 (ICAM-1), that facilitate the multistep leukocyte recruitment cascade (9–11). The steps of the recruitment process include tethering, rolling, firm adhesion, and transmigration into the extravascular space (7, 12). Leukocyte rolling is

[1] Correspondence: Angiogenesis Laboratory, 325 Cambridge St., 3rd Floor, Boston, MA 02114, USA. E-mail: ali_hafezi-moghadam@hms.harvard.edu

doi: 10.1096/fj.09-148981

0892-6638/10/0024-1532 © FASEB

mediated mainly through transient interaction of selectins with their ligands. The main selectin ligand, P-selectin glycoprotein ligand-1 (PSGL-1), is a 240-kDa disulfide-bonded homodimeric mucin-like glycoprotein, which is expressed on myeloid cells and a subset of lymphocytes (13). PSGL-1 binds to all three selectins (P-, E-, and L-selectin) and mediates leukocyte interaction with endothelial cells, platelets, and other leukocytes (14, 15). Under flow conditions, PSGL-1 interaction with P-selectin on the surface of activated endothelium mediates tethering and rolling (16, 17). ICAM-1, a member of the immunoglobulin superfamily, is constitutively expressed in leukocytes and endothelial cells (18). In uveitis, endothelial ICAM-1 expression is increased. ICAM-1 interaction with leukocyte integrins plays a key role in firm adhesion of rolling leukocytes (19, 20). LPS-induced ICAM-1 expression on endothelium is potently suppressed by corticosteroids, such as dexamethasone (dex; $IC_{50}<1$ nM) (21).

Previously, we showed up-regulation of endothelial P-selectin in live uveitic animals by using our custom-designed PSGL-1-conjugated MSs (6). However, PSGL-1-conjugated MSs target only one type of endothelial receptor, P-selectin, a mediator of rolling. *In vivo* expression of mediators of firm adhesion, such as ICAM-1 in living animals, remains to be studied.

In this work, we introduce novel molecular imaging agents that target two distinct types of endothelial surface molecules, a mediator of rolling and one that mediates firm adhesion, and evaluate the success of antiinflammatory treatment *in vivo*.

MATERIALS AND METHODS

Endotoxin-induced uveitis

All experiments were performed in accordance with the Association for Research in Vision and Ophthalmology (ARVO) Statement for the Use of Animals in Ophthalmic and Vision Research and were approved by the Animal Care and Use Committee of the Massachusetts Eye and Ear Infirmary. Male Lewis rats (8–10 wk old) were obtained from Charles River (Wilmington, MA, USA). Uveitis was induced in rats by injecting 100 μg of LPS (*Salmonella typhimurium*; Sigma Chemical, St. Louis, MO, USA) diluted in 0.1 ml sterile saline into one hind footpad of each animal (8). Control animals received a footpad injection of vehicle (saline). Animals were maintained in an air-conditioned room with a 12-h light-dark cycle and were given free access to water and food until used for the experiments.

Treatment

To reduce inflammation, animals were injected intraperitoneally with dex [5 mg/kg body weight (BW); American Regent, Inc. Shirley, NY, USA] (22, 23) 30 min before LPS. Control animals received an intraperitoneal injection of vehicle (saline).

MS preparation

Carboxylated fluorescent MSs (2 μm; Polysciences, Inc., Warrington, PA, USA) were covalently conjugated to protein G (Sigma), using a carbodiimide-coupling kit (Polysciences, Inc.) (7). MSs were incubated with nonimmune mouse IgG (mIgG; cat. no. 0102-14; Southern Biotech, Birmingham, AL, USA), anti-ICAM-1 (α-ICAM-1; Santa Cruz Biotechnology, Inc., Santa Cruz, CA, USA), recombinant PSGL-1 (rPSGL-1; Y's Therapeutics, Burlingame, CA, USA), or both α-ICAM-1 mAb and rPSGL-1 in equal quantities for 2 h at room temperature on a rotary shaker and subsequently washed with PBS and BSA (0.1%) (**Fig. 1**). Subsequently, MSs were washed again in PBS and sonicated before use *in vivo*. MSs (6×10^8) were injected into the tail vein of each animal.

Evaluation of MS rolling in the retinal and choroidal vessels

To evaluate MS rolling in the retinal vessel and the choriocapillaris in control and EIU animals, a scanning laser ophthalmoscope (SLO; HRA2; Heidelberg Engineering, Dossenheim, Germany), coupled with a computer-assisted image analysis system, was used to make continuous high-resolution fundus images. An argon blue laser was used as the excitation light, with a regular emission filter for fluorescein angiography, as the excitation (441 nm) and emission (488 nm) maxima of the MSs are comparable with those of sodium fluorescein. SLO images were obtained in a 30° angle at 15 frames/s and digitally recorded for further analysis. MSs were injected 24 h after LPS treatment, and images were recorded 30 min after MS injection.

Rats were anesthetized with xylazine hydrochloride (10 mg/kg) and ketamine hydrochloride (50 mg/kg), and their pupils were dilated with 0.5% tropicamide and 2.5% phenylephrine hydrochloride. A contact lens was used to retain corneal clarity throughout the experiment. Animals were placed on a platform, allowing flexible positioning of the animals in relation to the SLO. With a 30.5-gauge needle, MSs (6×10^8/ml in saline) were continuously injected intravenously into the tail vein within 60 s. Rolling MSs were defined as objects that moved at a significantly lower velocity than the free-flowing MSs. Velocity and number of rolling MSs were obtained from 30 s of the recordings.

Thirty minutes after the initial injection of the conjugated MSs, the numbers of free-flowing MSs in the retinal vessels and the choriocapillaris of control and EIU rats were substantially diminished, presumably due to the interaction of the MSs with the endothelium of the vessels throughout the body. This allowed us to conveniently identify and quantify the number of accumulated MSs in the retinal vessels and choriocapillaris as distinct stationary fluorescent marks with high contrast against the nonfluorescent background. ImageJ 1.41 software (National Institute of Health, Bethesda, MD, USA) was used for image analysis. For automated quantification of the number of bound microspheres in the choriocapillaris microvasculature, the confocal images were merged, and subsequently the area of the bright spots was measured in ImageJ 1.41.

Ex vivo evaluation of accumulated MSs and leukocytes

To prepare retinal and choroidal flatmounts, animals were anesthetized 24 h after LPS injection. Subsequently, 1 ml of MSs (6×10^8/ml in PBS) was injected continuously through the tail vein within 1 min. Thirty minutes after MS injection, animals were perfused with PBS (pH 7.4) and rhodamine-labeled concanavalin A lectin (RL-1002; Con-A; Vector Laboratories, Burlingame, CA, USA), 50 μg/ml in PBS (pH 7.4), to stain vascular endothelial cells and firmly adhering leukocytes. To perfuse the animals, the chest cavity was opened, and a 24-gauge needle was introduced

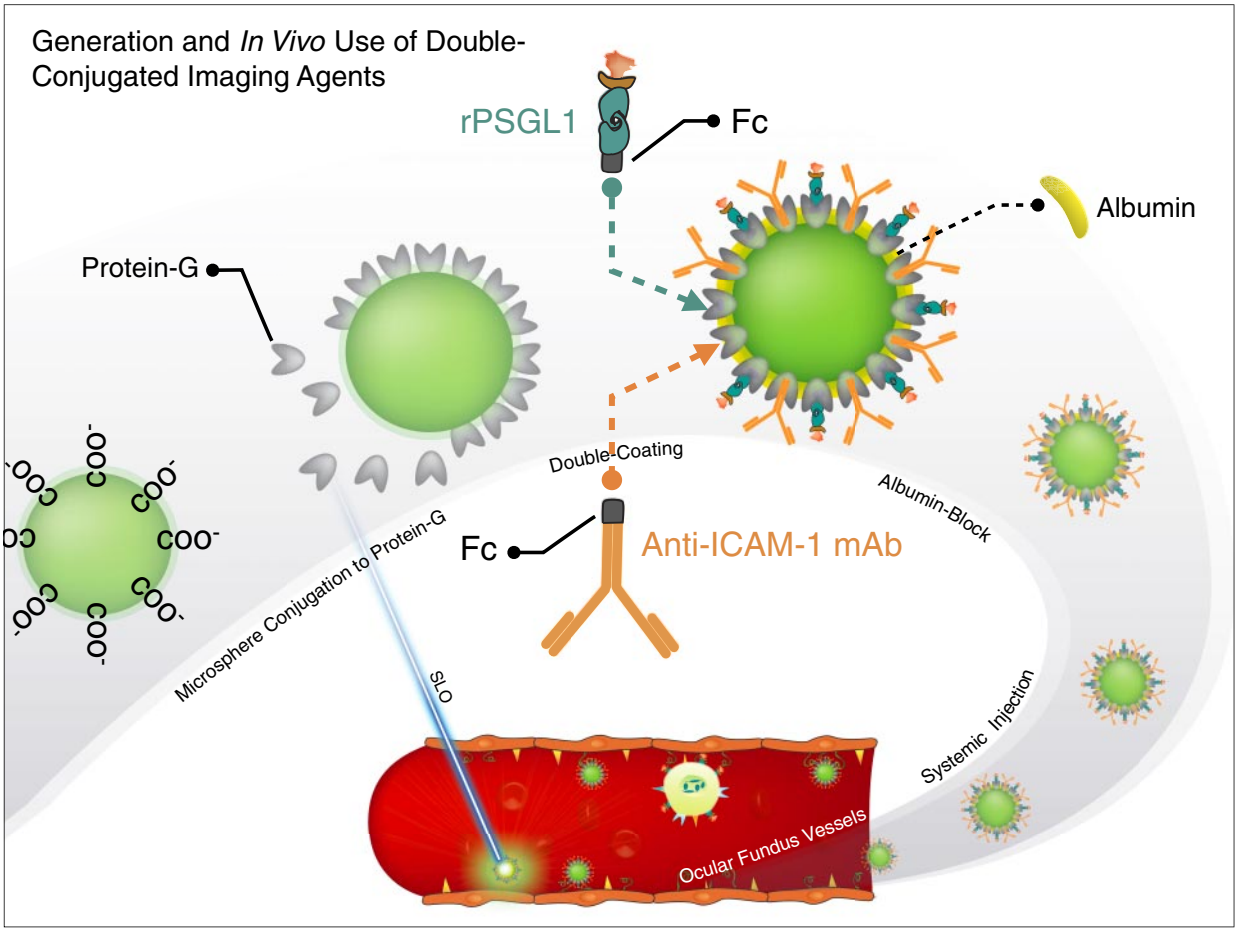

Figure 1. Schematic of our *in vivo* molecular imaging approach in the retinal and choroidal microcirculation. Fluorescent MSs, conjugated with α-ICAM-1 + rPSGL-1, are injected systemically in live animals. Retinal and choroidal microcirculation is imaged using SLO.

into the aorta. Drainage was achieved by opening the right atrium. PBS (50 ml) was injected to wash out intravascular content, including unbound MSs and leukocytes. This procedure was followed by perfusion with 0.3 ml ConA in 30 ml PBS to stain the vascular endothelium and firmly adhering leukocytes. Subsequently, 15 ml PBS was injected to wash out excess ConA. Immediately after perfusion, the retina and choroid were microdissected and flatmounted, using a fluorescence antifading medium (Vectashield, Vector Laboratories). The tissues were then observed under an epifluorescence microscope (DM RXA; Leica, Deerfield, IL, USA) with both an FITC (excitation, 488 nm; detection, 505–530 nm) and a rhodamine filter (excitation, 543 nm; detection, >560 nm). Images were obtained using a high-sensitivity digital camera, connected to a computer-assisted image analysis system. Using the Openlab™ image analysis software (Improvision, Boston, MA, USA), merged images of the MSs (green) with the retinal and the choroidal tissues (red) were generated. The numbers of firmly adhering leukocytes and MSs per surface area (mm^{-2}) in retinal arteries and veins and in the choriocapillaris were obtained by counting. In each preparation, micrographs (×10) from 5 different fields of view (optic disc, nasal, temporal, superior, and inferior) were obtained, and the leukocyte and microsphere numbers were counted and averaged. MSs that interacted with leukocytes *vs.* vascular endothelium were distinguished, and the percentage of MSs bound to leukocytes was calculated.

Statistical analysis

All values are expressed as means ± SE. Data were analyzed by Student's *t* test. Differences between the experimental groups were considered statistically significant or highly significant at values of $P < 0.05$ or 0.01, respectively.

RESULTS

MS rolling in retinal and choroidal vessels

To examine whether α-ICAM-1, rPSGL-1, or α-ICAM-1 + rPSGL-1 double-conjugated MSs roll in the fundus of EIU animals, we investigated these MSs *in vivo* using SLO. Immediately after intravenous injection of the various groups of conjugated MSs, free-flowing and rolling MSs were observed in the retinal vessels and the choriocapillaris of the examined rats (**Fig. 2*A***). In untreated control animals (n=6), only very few conjugated MSs rolled along the vascular endothelium of retinal vessels or choriocapillaris. In comparison, in EIU animals, 24 h after LPS injection, significantly more α-ICAM-1 + rPSGL-1 double-conjugated MSs rolled along the venous walls (retina: n=5, P=0.04; choroids: n=6, P=0.004) (Fig. 2*B*, C), suggesting increased levels of endothelial P-selectin and

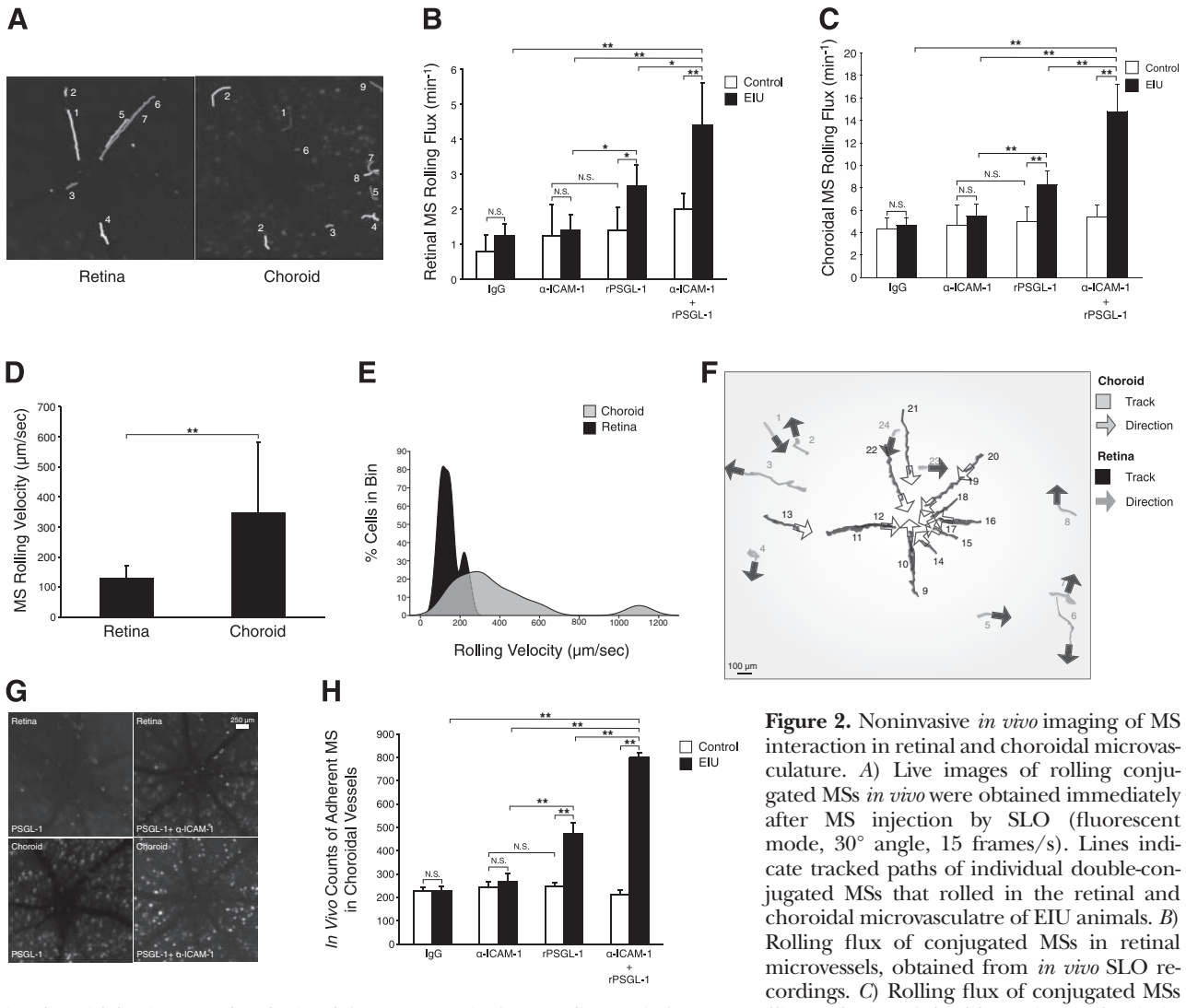

Figure 2. Noninvasive *in vivo* imaging of MS interaction in retinal and choroidal microvasculature. *A*) Live images of rolling conjugated MSs *in vivo* were obtained immediately after MS injection by SLO (fluorescent mode, 30° angle, 15 frames/s). Lines indicate tracked paths of individual double-conjugated MSs that rolled in the retinal and choroidal microvasculatre of EIU animals. *B*) Rolling flux of conjugated MSs in retinal microvessels, obtained from *in vivo* SLO recordings. *C*) Rolling flux of conjugated MSs in choroidal microvessels, obtained from *in vivo* SLO recordings. *D*) Average rolling velocity of double-conjugated MSs in retinal and choroidal vessels of EIU animals. *E*) Histogram of rolling velocities of double-conjugated MSs in retinal and choroidal vessels of EIU animals. *F*) Direction of rolling MSs in retinal and choroidal microvessels. In the retina, rolling MSs moved toward the optic disk, whereas in the choroid, MSs did not follow a uniform direction. Black lines, paths of individual MSs in retina; gray lines, paths of individual MSs in choroids. Arrows indicate direction of MS rolling in retina (open) and choroids (solid). *G*) Representative *in vivo* images showing MS accumulation in retinal and choroidal vessels of EIU animals. At 30 min after injection of conjugated MSs, SLO images were obtained in FA mode. White spots indicate firmly adhering MSs. *H*) Quantitative comparison of *in vivo* MS accumulation total area in choroidal vessels of an EIU animal, using SLO. MSs were conjugated with either IgG, α-ICAM-1, rPSGL-1, or both α-ICAM-1 + rPSGL-1. $*P < 0.05$; $**P < 0.01$.

ICAM-1 expression at these time points. Comparison of the rolling velocity of the double-conjugated MSs showed significantly higher values in the choroid (n=7) than in the retina (n=6; P=0.006) (Fig. 2*D*, *E*). In the retina, almost all rolling MSs were in the main vessels, and the direction of the rolling was from the periphery toward the optic disc. In contrast, in the choriocapillaris, MSs rolled in various directions (Fig. 2*F*).

MS accumulation in retinal and choroidal vessels

To investigate the expression of molecular indicators of injury in the ocular vessels, we quantified the areas of the bright spots in SLO micrographs as a measure of the number of adherent MSs in control and EIU animals. In control animals, all 4 differently conjugated MSs (n=5/group) showed low numbers of interaction with the endothelium of the choriocapillaris. In comparison, EIU animals showed significantly more accumulation of rPSGL-1 and double-conjugated MSs (IgG: n=5, P=0.9; α-ICAM-1: n=6, P=0.08; rPSGL-1: n=6, $P=6\times10^{-6}$; double-conjugated, n=6, $P=6.2\times10^{-11}$) 30 min after MS injection, especially in the central area and around the optic disc (Fig. 2*G*, *H*).

Ex vivo visualization of accumulated MSs

To confirm whether the conjugated MSs *in vivo* indeed adhered in the retinal and choriocapillaris vessels, as was evaluated based on the depth of focus in the *in vivo*

SLO experiments, we examined the accumulation of the conjugated MSs in perfused *ex vivo* tissue flatmounts. Using epifluorescence microscopy, we could confirm the adhesion of MSs and leukocytes in the retinal vessels (**Fig. 3*A–C***) and choriocapillaris (Fig. 3*D–F*). In line with our SLO findings, the flatmounts of α-ICAM-1, rPSGL-1, and double-conjugated MS-injected EIU animals showed significantly higher numbers of accumulation in retinal (n=6/group; $P_{\alpha\text{-ICAM-1}}$=0.01; $P_{\text{rPSGL-1}}$=0.0003; $P_{\text{double}}=2.6\times10^{-7}$) and choriocapillaris ($n$=6/group; $P_{\alpha\text{-ICAM-1}}=5.3\times10^{-12}$; $P_{\text{rPSGL-1}}=2.7\times10^{-13}$; $P_{\text{double}}=8.9\times10^{-15}$) than in the retinal and choriocapillaris vasculature of the controls (n=6/group). The binding of the mouse IgG-conjugated MSs to the retinal and choroidal vessels of EIU animals (n=6) did not differ from controls (n=5; retina: P=0.15; choroid: P=0.083).

The retinal flatmounts revealed that most of the firmly adhering MSs accumulated in the major retinal veins in all groups. Adhesion of α-ICAM-1 and rPSGL-1 single-conjugated MSs to the retinal vessels did not differ in control animals (n=6; P=0.4), whereas in EIU

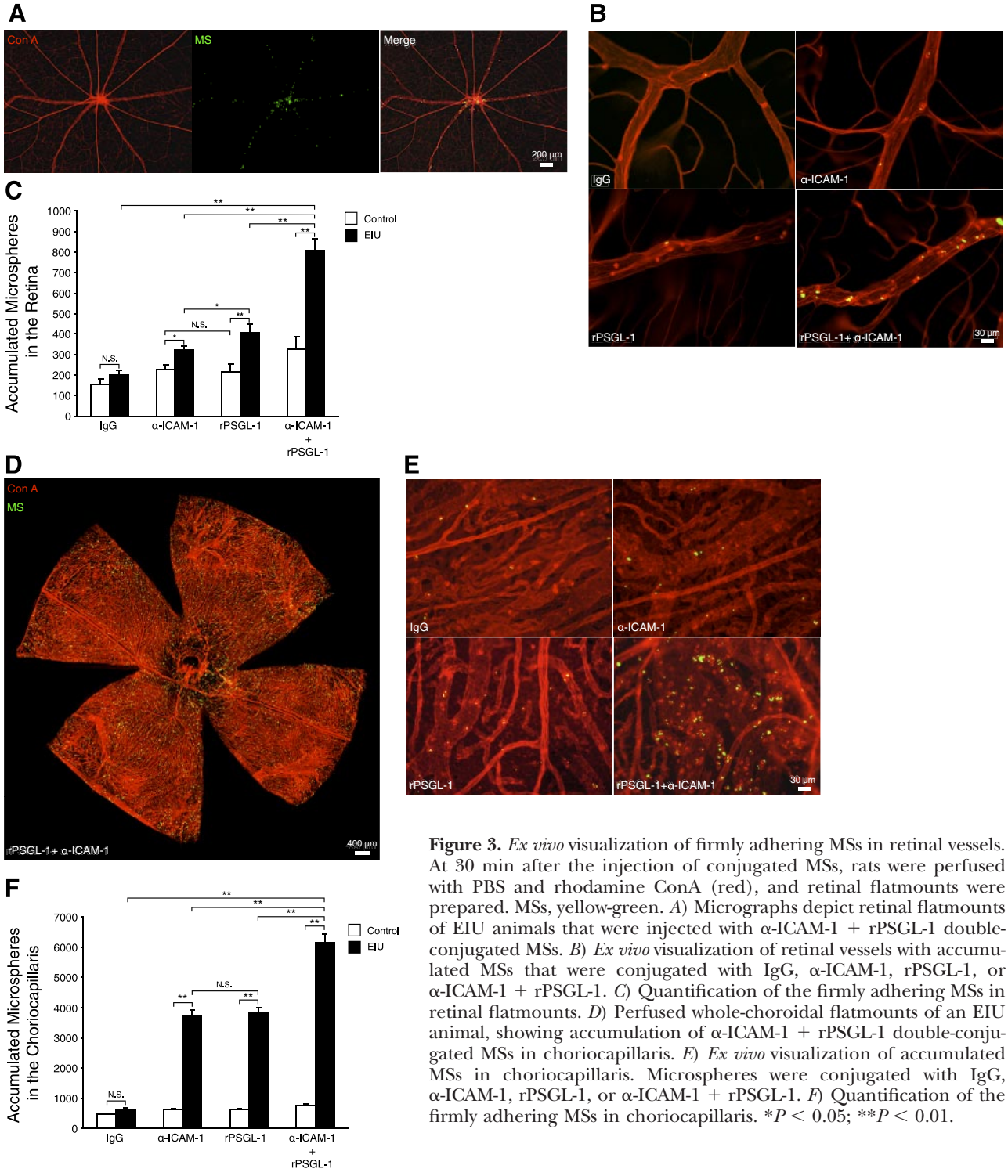

Figure 3. *Ex vivo* visualization of firmly adhering MSs in retinal vessels. At 30 min after the injection of conjugated MSs, rats were perfused with PBS and rhodamine ConA (red), and retinal flatmounts were prepared. MSs, yellow-green. *A*) Micrographs depict retinal flatmounts of EIU animals that were injected with α-ICAM-1 + rPSGL-1 double-conjugated MSs. *B*) *Ex vivo* visualization of retinal vessels with accumulated MSs that were conjugated with IgG, α-ICAM-1, rPSGL-1, or α-ICAM-1 + rPSGL-1. *C*) Quantification of the firmly adhering MSs in retinal flatmounts. *D*) Perfused whole-choroidal flatmounts of an EIU animal, showing accumulation of α-ICAM-1 + rPSGL-1 double-conjugated MSs in choriocapillaris. *E*) *Ex vivo* visualization of accumulated MSs in choriocapillaris. Microspheres were conjugated with IgG, α-ICAM-1, rPSGL-1, or α-ICAM-1 + rPSGL-1. *F*) Quantification of the firmly adhering MSs in choriocapillaris. *$P < 0.05$; **$P < 0.01$.

animals, rPSGL-1-conjugated MSs showed significantly higher adhesion than α-ICAM-1 (n=6, P=0.03). Furthermore, the numbers of double-conjugated MSs adhering to the retinal vessels of EIU animals were significantly higher than all other groups (IgG: n=5, $P=1.9\times10^{-9}$; α-ICAM-1: $P = 3\times10^{-7}$, n=6; rPSGL-1: n=6, $P = 2.7\times10^{-5}$) (Fig. 3*C*).

In the choroid, α-ICAM-1- and rPSGL-1-conjugated MSs did not show a significant difference in adhesion in the control and EIU groups (control n=6, P=0.9; EIU n=6, P=0.7). In control animals, significantly more double-conjugated MSs adhered to the choroidal flatmounts than to the singly conjugated MSs (α-ICAM-1: n=6, P=0.017; rPSGL-1: n=6, P=0.02). Also in choroidal flatmounts of the EIU animals, significantly more double-conjugated MSs adhered than single-conjugated MSs (α-ICAM-1: n=6, $P=2.7\times10^{-6}$; rPSGL-1: n=6, $P=3.8\times10^{-6}$) (Fig. 3*F*).

MS localization

To investigate whether the adhesion molecule-conjugated MSs are inside the vessels, we used confocal microscopy. The 3-D reconstruction of our flatmounts showed that all MSs were indeed in the vessels, both in the retina and the choroid with and without leukocytes (**Fig. 4*A***). These studies furthermore revealed that

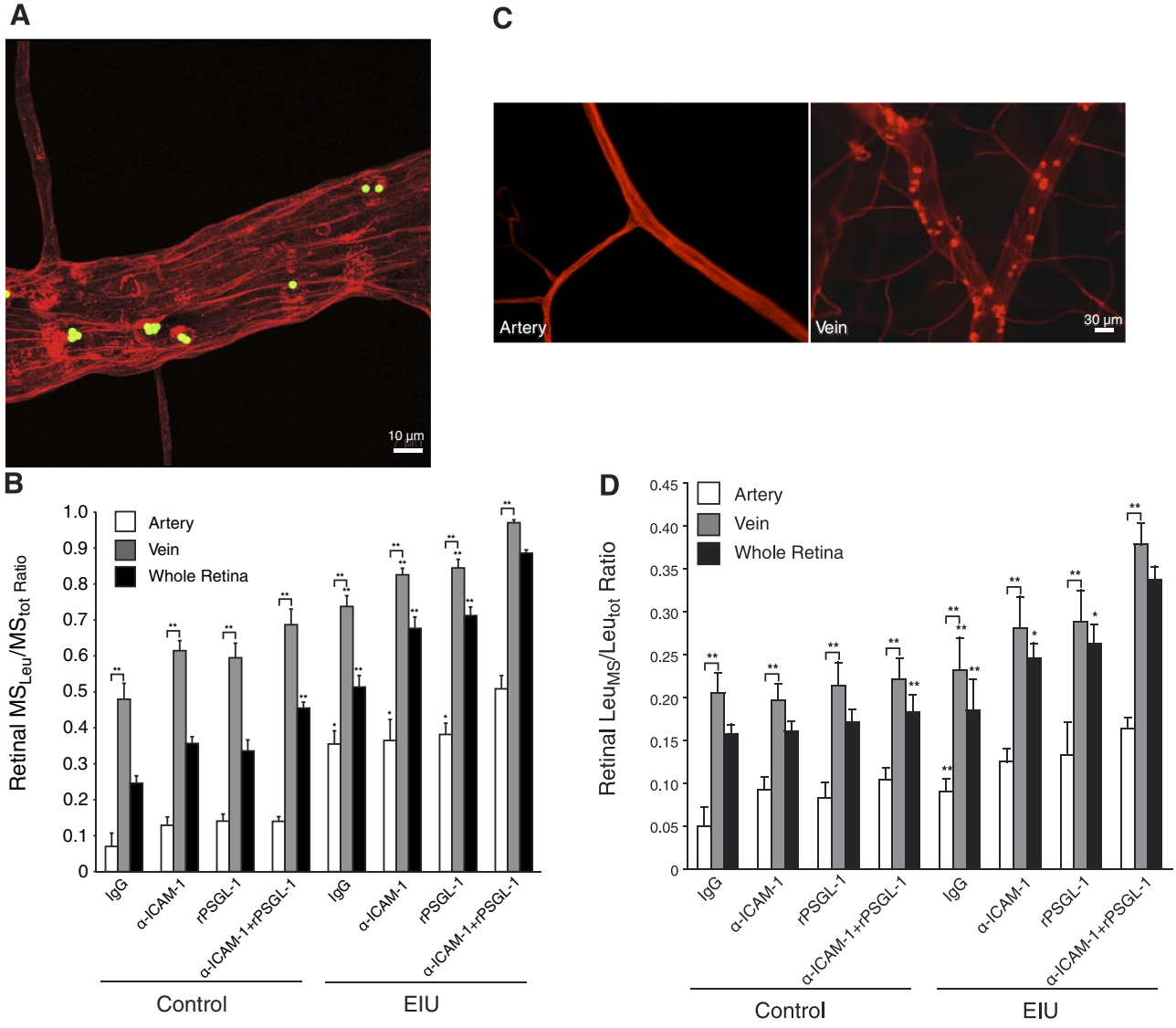

Figure 4. Conjugated MSs detect firmly adhering leukocytes. At 24 h after LPS treatment, Lewis rats were injected with MSs through the tail vein. At 30 min after MS injection, animals were perfused with PBS and rhodamine ConA to stain the vasculature and adherent leukocytes. Retinal and choroidal flatmounts of EIU animals were prepared. *A*) *Ex vivo* visualization of the accumulation of α-ICAM-1 + rPSGL-1 double-conjugated MSs in retina. Representative confocal laser micrograph depicts retinal flatmount of an EIU animal (3-D reconstruction of confocal sections, Supplemental Material). *B*) Ratio of MSs bound to leukocytes through number of MSs bound directly to endothelium (MS_{Leu}/MS_{tot}) in retinal arteries, veins, or whole retinal vasculature. *C*) *Ex vivo* visualization of firmly adherent leukocytes in retinal vessels of EIU animals. Micrographs show vasculature and firmly adhering leukocytes in retinal arteries and veins of animals injected with α-ICAM-1 + rPSGL-1 double-conjugated MSs. *D*) Ratio of numbers of leukocytes bound with MS/total number of firmly adherent leukocytes (Leu_{MS}/Leu_{tot}) in retinal arteries, veins, and whole retina. *$P < 0.05$; **$P < 0.01$.

some of the accumulated MSs directly bound to the vascular endothelium, while other MSs bound to firmly adhering leukocytes (Fig. 4*A*).

Visualization of accumulated leukocytes using conjugated MSs

To investigate the detection capability of our conjugated MSs for firmly adhering leukocytes, we calculated the ratio of MSs bound to leukocytes to the total number of accumulated MSs in the retinal vessels (MS_{Leu}/MS_{tot}). The MS_{Leu}/MS_{tot} ratio was obtained for retinal arteries, veins, and also total retinal vessels (Fig. 4*B*). In control animals, the comparison of the MS_{Leu}/MS_{tot} in arteries and veins, showed significantly higher ratios in veins (IgG: n=5, P=0.0001; α-ICAM-1: n=6, $P=9.3\times10^{-7}$; rPSGL-1: n=6, $P=8.2\times10^{-6}$; double-conjugated: n=6, $P=2.1\times10^{-6}$). Also, in EIU animals, MS_{Leu}/MS_{tot} ratios in veins were significantly higher than in arteries (IgG: n=5, $P=4.1\times10^{-5}$; α-ICAM-1: n=6, $P=6.8\times10^{-5}$; rPSGL-1: n=6, $P=2.7\times10^{-5}$; double: n=6, $P=4.0\times10^{-8}$). Furthermore, in EIU animals, the double-conjugated group showed significantly higher MS_{Leu}/MS_{tot} ratios compared with the single-conjugated groups in arteries (IgG: n=5, P=0.02, α-ICAM-1: n=6, P=0.048, rPSGL-1: n=6, P=0.03) and veins (IgG: n=5, $P=5.4\times10^{-6}$, α-ICAM-1: n=6, $P=1.1\times10^{-5}$, rPSGL-1: n=6, P=0.0002) and whole retinal vasculature (IgG: n=5, $P=1.5\times10^{-7}$, α-ICAM-1: n=6, $P=2.6\times10^{-5}$, rPSGL-1: n=6, $P=1.84\times10^{-5}$).

In retinal veins of EIU animals that were injected with conjugated MSs, we found the highest number of single-conjugated MSs bound with one leukocyte to be 8 (1.5±1.6, n=20 leukocytes). In comparison, in the double-conjugated group, significantly more MSs, up to 15, bound with one adhering leukocyte (5.7±2.5 MS/leukocyte, n=20 leukocytes, $P=1.6\times10^{-5}$), indicating more effective detection of firmly adhering leukocytes with double-conjugated MSs. In line with the MS binding data, in the retina of EIU animals, most adherent leukocytes were in the veins, and very few in arteries or in retinal capillaries (>3rd degree vessels) (Fig. 4*C*).

To learn about the efficacy of the conjugated MSs in detecting firmly adhering leukocytes, we calculated the ratio of leukocytes bound with MS/total firmly adherent leukocytes (Leu_{MS}/Leu_{tot}) in retinal arteries, veins, and the whole retina. The Leu_{MS}/Leu_{tot} ratio was significantly higher in veins compared to arteries, both in control (n=5–6; P_{IgG}=0.001, $P_{\alpha\text{-ICAM-1}}$=0.002, $P_{rPSGL\text{-}1}$=0.004, P_{double}=0.002) and EIU animals (n=5–6; P_{IgG}=0.01, $P_{\alpha\text{-ICAM-1}}$=0.003, $P_{rPSGL\text{-}1}$=0.002, $P_{double}=5.5\times10^{-6}$). In EIU animals ($n$=5–6), the double-conjugated MS showed significantly higher Leu_{MS}/Leu_{tot} ratios than IgG-conjugated MSs in arteries (P_{IgG}=0.005, $P_{\alpha\text{-ICAM-1}}$=0.09, $P_{rPSGL\text{-}1}$=0.4) and veins (P_{IgG}=0.007, $P_{\alpha\text{-ICAM-1}}$=0.08, $P_{rPSGL\text{-}1}$=0.06), than all of the other 3 groups in the whole retina (P_{IgG}=0.003, $P_{\alpha\text{-ICAM-1}}$=0.01, $P_{rPSGL\text{-}1}$=0.02) (Fig. 4*D*).

Noninvasive molecular evaluation of antiinflammatory treatment

To investigate the potential of our molecular imaging approach in evaluation of antiinflammatory interventions, we treated EIU animals with dex and imaged the interaction of conjugated MSs with retinal and choroidal vessels. The quantification of our SLO images indicates that in dex-treated EIU animals significantly fewer MSs adhered to the choroidal vessels compared to the untreated EIU group (n=6/group, $P=6.3\times10^{-9}$) (**Fig. 5*A*, *B***). In flatmounts, dex-treated animals showed significantly lower rates of MS adhesion in the retina (n=6, $P=9.0\times10^{-10}$) and choroid (n=6, $P=2.0\times10^{-11}$) than untreated animals (Fig. 5*C*, *D*). Consistent with the antiinflammatory function of steroids, the numbers of firmly adherent leukocytes were significantly lower in retinas of dex-treated EIU animals than untreated controls, both in arteries ($P=1.6\times10^{-10}$) and veins ($P=10^{-10}$) (Fig. 5*E*). The comparison of leukocyte adhesions in the choriocapillaris showed significantly lower numbers in the dex-treated (n=6) than in untreated EIU animals (n=6, $P=10^{-7}$) (Fig. 5*F*, *G*).

The MS_{Leu}/MS_{tot} ratio was significantly lower in the dex-treated animals (n=6) compared to the untreated controls (n=6), in arteries ($P=2.6\times10^{-5}$), veins ($P=5.5\times10^{-6}$), or in the whole retinas ($P=9.8\times10^{-8}$) (Fig. 5*H*). Similarly, the Leu_{MS}/Leu_{tot} ratio was significantly lower in the dex-treated animals (n=6) compared to the untreated controls (n=6); in arteries (P=0.004), veins (P=0.002), or in the whole retinas (P=0.002) (Fig. 5*I*).

DISCUSSION

Noninvasive detection of molecular events in the living organism can revolutionize medicine. The eye provides a unique portal for visible-light-based imaging of retinal and choroidal microvessels. Recently, we introduced noninvasive imaging of endothelial injury in the fundus vessels (6). This work introduces and characterizes a new imaging agent that simultaneously targets two different classes of endothelial markers, a rolling and an adhesion receptor.

Our results show the superior sensitivity of double-conjugated MSs for detection of endothelial injury, compared to MSs that only target one type of endothelial markers. Our previous work showed accumulation of rPSGL-1-conjugated MSs in choroidal microvessels (6). Here, we also quantitatively compare the rolling of various MSs in retinal and choroidal vessels. The rolling flux of rPSGL-1-conjugated MSs is significantly higher in EIU animals than in controls. In contrast, the rolling flux of α-ICAM-1-conjugated MSs is not significantly different between EIU and control animals. This finding is in line with the fact that CD18/ICAM-1 is not primarily a rolling ligand pair *in vivo*. The significantly higher rolling interaction of the double-conjugated MSs compared to the rPSGL-1-conjugated MSs indicates that ICAM-1 may contribute to the rolling of the MSs, once the interaction with the endothelium is initiated.

Surprisingly, the rolling velocity of the double-conjugated MSs is significantly higher in the choroidal vessels than in the retina. The absolute number of MS interactions in the choriocapillaris is higher than in the retina. This difference might be explained by the higher vascular density in the choriocapillaris com-

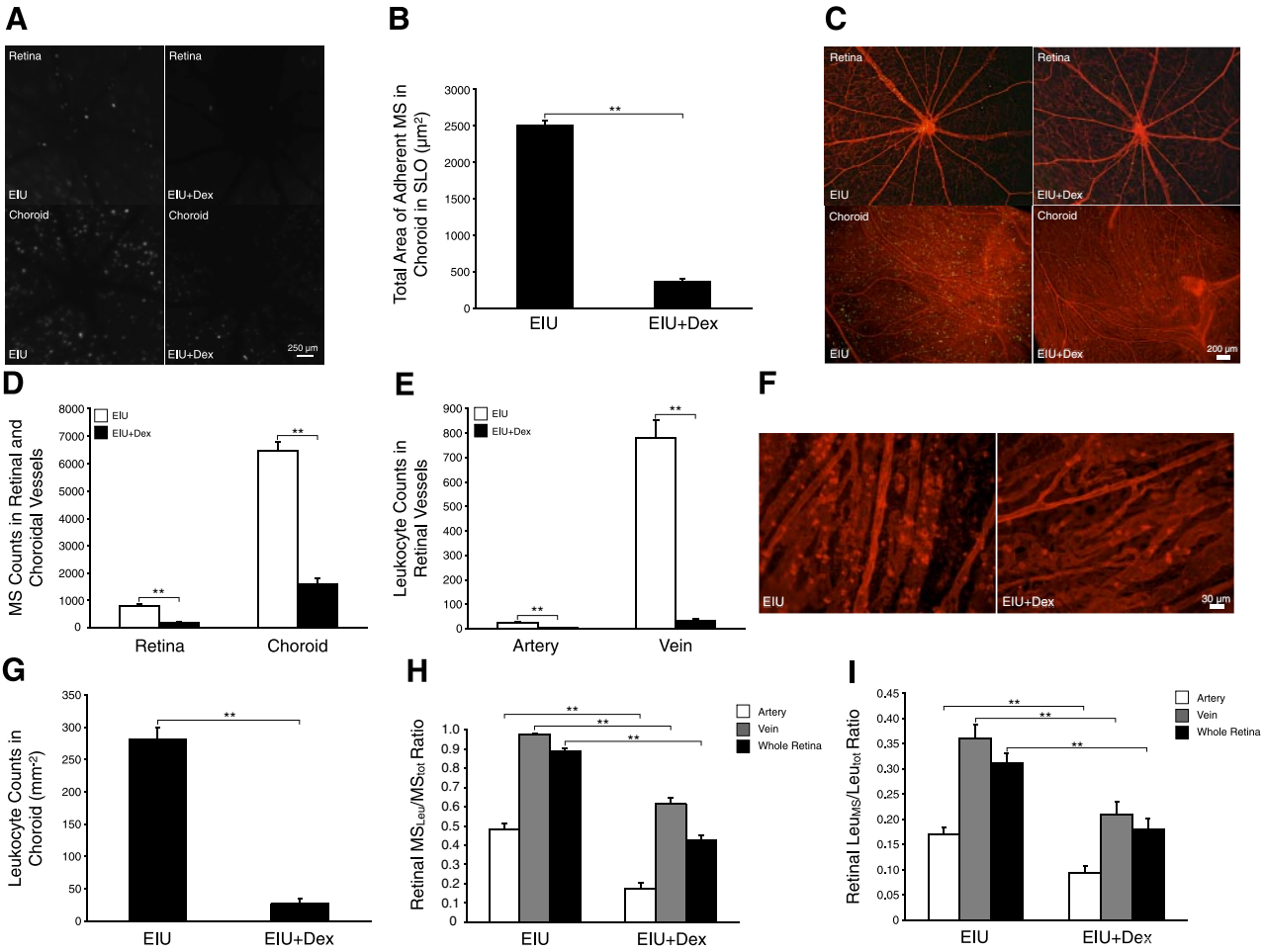

Figure 5. *In vivo* molecular evaluation of antiinflammatory treatment success. Representative micrographs of retinal and choroidal vessels *in vivo* (SLO) and *ex vivo* (flatmounts) in EIU animals, 24h after LPS treatment. Adhesion molecule-conjugated MSs were injected through the tail vein. For *ex vivo* preparations, animals were perfused with rhodamine ConA to stain the vasculature and adherent leukocytes. *A*) *In vivo* SLO images of accumulated MSs in retinal and choroidal microvessels of vehicle- or dex-treated EIU animals. White spots, firmly adhering MSs in retinal and choriocapillaris vasculature. *B*) Quantitative comparison of *in vivo* MS accumulation in choroidal vessels using SLO. *C*) *Ex vivo* visualization of accumulation of α-ICAM-1 + rPSGL-1 double-conjugated MSs in retina and choroid of EIU animals with or without dex treatment. *D*) Accumulation of α-ICAM-1 + rPSGL-1 double-conjugated MSs in retinal and choroidal flatmounts of EIU animals with or without dex treatment. *E*) Quantitative comparison of accumulation of firmly adherent leukocytes in retinal arteries and veins of EIU animals with or without dex treatment. *F*) *Ex vivo* visualization of accumulation of leukocytes in choriocapillaris of EIU animals with or without dex treatment. *G*) Quantitative comparison of accumulated leukocytes in choriocapillaris (mm^{-2}). *H*) Ratio of MSs bound to leukocytes through number of MSs bound to endothelium vessels (MS_{Leu}/MS_{tot}) in EIU animals with or without dex treatment in arteries, veins, or entire vasculature. *I*) Ratio of numbers of leukocytes bound with MS/total firmly adherent leukocytes (Leu_{MS}/Leu_{tot}) in retinas of EIU animals with or without dex treatment in retinal arteries, veins, or whole vasculature. $^{**}P < 0.01$.

pared to the retina. Also, the inflammatory response in the choroid may differ from retina. Another striking qualitative difference between the two vascular beds is that in the retina, most rolling initiates from the periphery and continues toward the optic nerve head, suggesting that the rolling interaction mainly occurs in the retinal veins. In contrast, in the choriodal vasculature, the direction of rolling is variable, conforming to the network structure of the choriocapillaris.

Beyond direct detection of endothelial injury, it would be highly desirable to detect accumulated immune cells in the retinal or choroidal vessels. MSs conjugated with rPSGL-1 or α-ICAM-1 bind to firmly adhering leukocytes, as leukocytes express L-selectin (binding partner of PSGL-1) as well as ICAM-1. Double-conjugated MSs bind in significantly higher numbers to firmly adhering leukocytes, making them more effective in targeting immune cells than singly conjugated MSs. To better understand the binding of the imaging agents to the vasculature *vs.* to firmly adhering leukocytes, we built the MS_{Leu}/MS_{tot} and Leu_{MS}/Leu_{tot} ratios. The MS_{Leu}/MS_{tot} shows specificity of the various conjugated MSs for firmly adhering leukocytes and distinguishes MS binding directly to the leukocyte, compared to the total MS binding. The double-conjugated MSs show higher binding ratios to leukocytes, suggesting their superior detection capability for firmly adhering leukocytes. In comparison, the Leu_{MS}/Leu_{tot}

ratio shows the percentage of firmly adhering leukocytes that are detected by MSs, providing potentially valuable insights into the subpopulation of the leukocytes that are being detected. In both ratios, doubly conjugated MSs show significantly higher values than the singly conjugated MSs. Also, in both ratios, veins show significantly higher values than arteries, suggesting that hemodynamic differences (*i.e.*, differences in shear rates) may affect MS binding to leukocytes more than to the endothelium. The fact that leukocytes preferentially accumulate in veins supports the hypothesis that our molecule-conjugated MSs mimic the pathophysiologically relevant phenomenon of leukocyte recruitment in EIU.

Our noninvasive molecular imaging approach can be used for follow up of treatment success. We show that accumulation of adhesion molecule-conjugated MSs correlates well with the degree of the endothelial injury during antiinflammatory treatment. Dex treatment inhibits MS rolling and adhesion, similar to the effect it has on leukocyte recruitment. This indicates that MS binding correlates with the degree of inflammation and provides insights about its resolution.

In sum, the present work introduces a novel imaging approach that advances our *in vivo* detection capabilities to the cellular and molecular level. Besides being a powerful research tool, this versatile imaging approach has a high chance of being translated to the clinical realm and affecting the way medicine is practiced. FJ

Recombinant PSGL-1 (Y's PSGL) was a generous gift of Y's Therapeutics, Inc. (San Bruno, CA, USA). The authors thank Mark I. Melhorn and Rebecca C. Garland for their help in the preparation of this manuscript. This work was supported by U.S. National Institute of Health (NIH) grants AI050775 (A.H.-M.) and HL086933 (Alan Cross, University of Maryland, College Park, MD, USA), the American Health Assistance Foundation (A.H.-M.), and a Science and Technology project of Heilongjiang Province, China (GB06C40104 to D.S.). The authors thank the Massachusetts Lions Eye Research Fund Inc., Research to Prevent Blindness, and the Marion W. and Edward F. Knight AMD Fund. Author contributions: A.H.-M. designed research; D.S., S.N., F.X., and S.Z. performed research; D.S., A.S., and A.H.-M. analyzed data; D.S. and A.H.-M. wrote the paper.

REFERENCES

1. Durrani, O. M., Meads, C. A., and Murray, P. I. (2004) Uveitis: a potentially blinding disease. *Ophthalmologica* **218,** 223–236
2. Hafezi-Moghadam, A., Noda, K., Almulki, L., Iliaki, E. F., Poulaki, V., Thomas, K. L., Nakazawa, T., Hisatomi, T., Miller, J. W., and Gragoudas, E. S. (2007) VLA-4 blockade suppresses endotoxin-induced uveitis: in vivo evidence for functional integrin up-regulation. *FASEB J.* **21,** 464–474
3. Bischoff, P. M., Niederberger, H. J., Torok, B., and Speiser, P. (1995) Simultaneous indocyanine green and fluorescein angiography. *Retina* **15,** 91–99
4. Hirata, Y., and Nishiwaki, H. (2006) The choroidal circulation assessed by laser-targeted angiography. *Prog. Retin. Eye Res.* **25,** 129–147
5. Khoobehi, B., Shoelson, B., Zhang, Y. Z., and Peyman, G. A. (1997) Fluorescent microsphere imaging: a particle-tracking approach to the hemodynamic assessment of the retina and choroid. *Ophthalmic. Surg. Lasers* **28,** 937–947
6. Miyahara, S., Almulki, L., Noda, K., Nakazawa, T., Hisatomi, T., Nakao, S., Thomas, K. L., Schering, A., Zandi, S., Frimmel, S., Tayyari, F., Garland, R. C., Miller, J. W., Gragoudas, E. S., Masli, S., and Hafezi-Moghadam, A. (2008) In vivo imaging of endothelial injury in choriocapillaris during endotoxin-induced uveitis. *FASEB J.* **22,** 1973–1980
7. Hafezi-Moghadam, A., Thomas, K. L., Prorock, A. J., Huo, Y., and Ley, K. (2001) L-selectin shedding regulates leukocyte recruitment. *J. Exp. Med.* **193,** 863–872
8. Rosenbaum, J. T., McDevitt, H. O., Guss, R. B., and Egbert, P. R. (1980) Endotoxin-induced uveitis in rats as a model for human disease. *Nature* **286,** 611–613
9. Suzuma, K., Mandai, M., Kogishi, J., Tojo, S. J., Honda, Y., and Yoshimura, N. (1997) Role of P-selectin in endotoxin-induced uveitis. *Invest. Ophthalmol. Vis. Sci.* **38,** 1610–1618
10. Miyamoto, K., Ogura, Y., Hamada, M., Nishiwaki, H., Hiroshiba, N., and Honda, Y. (1996) In vivo quantification of leukocyte behavior in the retina during endotoxin-induced uveitis. *Invest. Ophthalmol. Vis. Sci.* **37,** 2708–2715
11. Devine, L., Lightman, S. L., and Greenwood, J. (1996) Role of LFA-1, ICAM-1, VLA-4 and VCAM-1 in lymphocyte migration across retinal pigment epithelial monolayers in vitro. *Immunology* **88,** 456–462
12. Hafezi-Moghadam, A., and Ley, K. (1999) Relevance of L-selectin shedding for leukocyte rolling in vivo. *J. Exp. Med.* **189,** 939–948
13. Laszik, Z., Jansen, P. J., Cummings, R. D., Tedder, T. F., McEver, R. P., and Moore, K. L. (1996) P-selectin glycoprotein ligand-1 is broadly expressed in cells of myeloid, lymphoid, and dendritic lineage and in some nonhematopoietic cells. *Blood* **88,** 3010–3021
14. Spertini, O., Cordey, A. S., Monai, N., Giuffre, L., and Schapira, M. (1996) P-selectin glycoprotein ligand 1 is a ligand for L-selectin on neutrophils, monocytes, and CD34+ hematopoietic progenitor cells. *J. Cell Biol.* **135,** 523–531
15. Moore, K. L. (1998) Structure and function of P-selectin glycoprotein ligand-1. *Leuk. Lymphoma* **29,** 1–15
16. Norman, K. E., Moore, K. L., McEver, R. P., and Ley, K. (1995) Leukocyte rolling in vivo is mediated by P-selectin glycoprotein ligand-1. *Blood* **86,** 4417–4421
17. Geng, J. G., Bevilacqua, M. P., Moore, K. L., McIntyre, T. M., Prescott, S. M., Kim, J. M., Bliss, G. A., Zimmerman, G. A., and McEver, R. P. (1990) Rapid neutrophil adhesion to activated endothelium mediated by GMP-140. *Nature* **343,** 757–760
18. Xu, H., Forrester, J. V., Liversidge, J., and Crane, I. J. (2003) Leukocyte trafficking in experimental autoimmune uveitis: breakdown of blood-retinal barrier and upregulation of cellular adhesion molecules. *Invest. Ophthalmol. Vis. Sci.* **44,** 226–234
19. Kanagawa, T., Matsuda, S., Mikawa, Y., Kogiso, M., Nagasawa, H., Himeno, K., Hashimoto, Y., and Mimura, Y. (1996) Role of ICAM-1 and LFA-1 in endotoxin-induced uveitis in mice. *Jpn. J. Ophthalmol.* **40,** 174–180
20. Becker, M. D., Garman, K., Whitcup, S. M., Planck, S. R., and Rosenbaum, J. T. (2001) Inhibition of leukocyte sticking and infiltration, but not rolling, by antibodies to ICAM-1 and LFA-1 in murine endotoxin-induced uveitis. *Invest. Ophthalmol. Vis. Sci.* **42,** 2563–2566
21. Cronstein, B. N., Kimmel, S. C., Levin, R. I., Martiniuk, F., and Weissmann, G. (1992) A mechanism for the antiinflammatory effects of corticosteroids: the glucocorticoid receptor regulates leukocyte adhesion to endothelial cells and expression of endothelial-leukocyte adhesion molecule 1 and intercellular adhesion molecule 1. *Proc. Natl. Acad. Sci. U. S. A.* **89,** 9991–9995
22. Jin, X. H., Ohgami, K., Shiratori, K., Suzuki, Y., Hirano, T., Koyama, Y., Yoshida, K., Ilieva, I., Iseki, K., and Ohno, S. (2006) Inhibitory effects of lutein on endotoxin-induced uveitis in Lewis rats. *Invest. Ophthalmol. Vis. Sci.* **47,** 2562–2568
23. Nakao, S., Hata, Y., Miura, M., Noda, K., Kimura, Y. N., Kawahara, S., Kita, T., Hisatomi, T., Nakazawa, T., Jin, Y., Dana, M. R., Kuwano, M., Ono, M., Ishibashi, T., and Hafezi-Moghadam, A. (2007) Dexamethasone inhibits interleukin-1beta-induced corneal neovascularization: role of nuclear factor-kappaB-activated stromal cells in inflammatory angiogenesis. *Am. J. Pathol.* **171,** 1058–1065

Received for publication October 20, 2009.
Accepted for publication December 3, 2009.